CAUCHY – Jurnal Matematika Murni dan Aplikasi
Volume 11 (1) (2026), Pages 556-570
p-ISSN: 2086-0382; e-ISSN: 2477-3344

Infection Clearance Rate in Fractional-Order SEIR Model: Stability Analysis

Muhammad Iqbal, Mohammad Januar Ismail Burhan*, and Adam

Department of Mathematics, Faculty of Science and Information Technology, Institut Teknologi Kalimantan, Indonesia

Abstract

Infectious disease has become a serious problem over the past few years. At the same time, research on disease dynamics keeps advancing, especially on diseases caused by viruses. One concept that has been used in epidemic models is fractional calculus, or more specifically, fractional differential equations. This paper discusses the analytical properties of a fractional-order SEIR model, which are then verified by numerical simulations. Fractional-order has the property of memory effect, which represents the past experience effect on the current behavior of people. Mathematically, the present state is affected by previous states. Analytical results have shown that fractional-order value does not change the stability condition for each equilibrium. It is shown that there exists a stronger sufficient condition for disease-free equilibrium to be globally asymptotically stable. For the endemic equilibrium, it is only proven to be locally asymptotically stable when the basic reproduction number is greater than 1. Simulation results from Explicit Fractional Order Runge–Kutta (EFORK) method are confirmed to be in agreement with the basic properties provided by the analysis. The results also illustrate the impact of fractional-order and infection clearance rate, indicating that smaller fractional-orders converge faster compared to larger orders.

Keywords: Fractional-order; Infection Clearance Rate; SEIR Model; Stability Analysis.

1. Introduction

Infectious diseases have been an issue at many different times throughout the history of humanity. World Health Organization (WHO) reported that three major causes of death globally in 2021 were infectious diseases. The three diseases are COVID-19, lower respiratory infections, and tuberculosis. COVID-19, as the most recent disease, took 8.8 million lives in 2021. Furthermore, in low-income countries, malaria and HIV/AIDS are also among the ten major causes of death [1]. There are also other infectious diseases that can cause an outbreak, such as the sudden mpox outbreak in 2022, which spread rapidly in Europe, America, and all six WHO regions [2]. In response to this issue, studies on infectious disease dynamics have been increasing in recent years.

Research on disease dynamics dates back to 1927, when Kermack and McKendrick developed a mathematical model capable of describing disease dynamics by categorizing the population into three different compartments: susceptible, infected, and recovered. This model, known as the SIR model, serves as a foundation in many studies of various diseases, which are then modified

*Corresponding author. E-mail: januarismail@lecturer.itk.ac.id

Submitted: February 02, 2026 Reviewed: February 08, 2026 Accepted: March 04, 2026
DOI: https://doi.org/10.18860/cauchy.v11i1.40849

with different formulas and assumptions [3], [4], [5], [6]. One of the advancements of the SIR model is the implementation of the memory effect with fractional calculus. In comparison to integer-order, fractional-order presents an additional parameter when fitting the model to real data [7]. Models that are closer to real data can give insights on how the disease spreads, such as the values of transmission and recovery rates, thereby aiding in the process of preventing disease outbreaks. In this study, we will discuss a modification on the SIR model in [8], which is a SEIR model. This research aims to analyze the basic properties of a fractional-order SEIR model with an infection clearance rate parameter, where people recover with no acquired immunity post-infection.

Following the past research, we will use the Caputo definition of fractional derivative from the many established definitions in fractional calculus. A simple formula of a fractional-order SIR model is given by

$$\begin{aligned} D^\alpha S &= -\beta^\alpha SI, \\ D^\alpha I &= \beta^\alpha SI - \tau^\alpha I, \\ D^\alpha R &= \tau^\alpha I. \end{aligned}$$

where D^α is the Caputo fractional derivative operator with the fractional-order $\alpha \in (0,1)$. Parameters such as β and τ have an exponent of α because the dimension of D^α is $(time)^{-\alpha}$ [7]. Other works simplify the writing of the formula without the exponent α, but essentially all parameter's dimension is still $(time)^{-\alpha}$.

Fractional-order α has the concept of memory effects, which represents how past experiences influence the current behavior of people. Mathematically, the present state of a system is affected by its previous states. Models with fractional-order are generally closer to the actual data [7]. Thus, epidemic models with fractional-order have become a topic of discussion in epidemiology. There are a number of research, including those that take into account the possibility of reinfection [8], [9].

The basic assumption of SIR epidemic model is that a previously infected individual will recover naturally after a period of time and gain permanent immunity. However, there are diseases that are able to infect an individual more than once either because the immunity to those diseases is only temporary or there is no post-infection immunity. This particular assumption is implemented in one of the studies regarding the fractional-order SIR model. The study has shown that a smaller fractional-order results in faster convergence towards equilibrium state. Additionally, increasing the value of treatment cure rate effectively reduces the number of infected people [8].

We will then proceed to carry out this idea in the fractional-order SEIR model below.

$$\begin{aligned} D^\alpha S &= \Lambda - (\mu+\gamma)S - \beta SI + \omega I, \\ D^\alpha E &= \beta SI - (\delta+\mu)E, \\ D^\alpha I &= \delta E - (\tau+\mu+\omega)I, \\ D^\alpha R &= \gamma S + \tau I - \mu R, \end{aligned} \tag{1}$$

where $\alpha \in (0,1]$. S, E, I, and R represent the susceptible, exposed, infected, and recovered individuals separately. The initial values ($S(0)$, $E(0)$, $I(0)$, $R(0)$) and all parameters are assumed to be nonnegative. Parameters used in the model include Λ as the population growth rate, μ as the mortality rate, β as the transmission rate, γ as the vaccination rate, δ as the rate of transition from E to I, τ as the rate of transition from I to R, and ω as the infection clearance rate. Individuals in compartment R are those who have received permanent immunity, either from vaccination or as an aftermath after recovery. However, individuals in compartment I could become susceptible as soon as the infection is cleared up. In this case, the individual returns to compartment S. Additionally, infection is caused by physical contact or close-distance interaction with individuals in compartment I. This means that people in compartment E cannot spread the disease.

We present some properties used in this research, such as the definition, lemma, and theorem in Section 2. The basic analytical properties of the model are presented in Section 3, starting from nonnegativity and boundedness of solution to the stability analysis of equilibrium points. Additionally, numerical simulations are also presented in Section 3 to support the analytical results. Finally, we conclude the results of this research in Section 4.

2. Methods

As stated in the Introduction, the goal is to find the analytical properties of the fractional SEIR model in Eq. (1) and verify it by running numerical simulations. To preface, we must introduce some mathematical statements from previous research. As mentioned before, below is the Caputo definition of the fractional derivative.

Definition 1. [10] Caputo fractional derivative of the function $h : \mathbb{R}^+ \to \mathbb{R}$ with respect to α is defined by

$$D^\alpha h(t) = \frac{1}{\Gamma(n-\alpha)} \int_0^t (t-p)^{n-\alpha-1} \frac{d^n h(p)}{dp^n}, \; n-1 < \alpha \leq n$$

To analyze the nonnegativity and boundedness of the solution, we introduce the following Lemmas 2–5.

Lemma 2. *[8] Suppose that a system of fractional differential equations is given by*

$$D^\alpha W(t) = G(W), W(0) = W_0$$

where $G : \mathbb{R}^n \to \mathbb{R}^n$, $n \in \mathbb{N}$, $0 < \alpha \leq 1$, and $W_0 \in \mathbb{R}^n$. If the two conditions below are satisfied, which are

1. *$G(W)$ and $\frac{\partial}{\partial W} G(W)$ are continuous in $\mathbb{R}^n$, and*
2. *$||G(W)|| \leq u_1 + u_2||W||$ for all $W \in \mathbb{R}^n$ such that $u_1, u_2 > 0$,*

then the system has a unique solution for all $t \in [0, \infty)$.

Lemma 3. *[11] Let $h(t)$ and its fractional derivative $D^\alpha h(t)$ be continuous functions on $[a, b]$ where $\alpha \in (0, 1]$. There exist $h(t)$ such that for every $t \in (a, b]$,*

$$h(t) = h(a) + \frac{1}{\Gamma(\alpha)} D^\alpha g(\zeta)(t-a)^\alpha, a < \zeta < t$$

Lemma 4. *[11] Let $h(t)$ and its fractional derivative $D^\alpha h(t)$ be continuous functions on $[a, b]$ where $\alpha \in (0, 1]$. If $D^\alpha h(t)$ is nonnegative for all $t \in [a, b]$, then $h(t)$ is nondecreasing on $[a, b]$. Conversely, if $D^\alpha h(t)$ is nonpositive for all $t \in [a, b]$, then $h(t)$ is nonincreasing on $[a, b]$.*

Lemma 5. *[12] The Laplace transformation of $D^\alpha h(t)$ is given by*

$$\mathcal{L}\{D^\alpha h(t)\} = s^\alpha \mathcal{L}\{h(t)\} - s^{\alpha-1} h(0).$$

For equilibrium points and local stability analysis, we present Lemma 6 below.

Lemma 6. *[9] Consider the system of fractional differential equations given by*

$$D^{\alpha}\vec{h}(t) = \Phi(\vec{h}),\ \vec{h}(t) = (h_1(t_0), h_2(t_0), ..., h_n(t_0)),$$

where $\alpha \in (0,1]$, $\vec{h} = (h_1, h_2, ..., h_n)$, *and* $\Phi(\vec{h}) : [t_0, \infty] \to \mathbb{R}^{n\times n}$. *The solutions of* $\Phi(\vec{h}) = \vec{0}$ *are the equilibrium points. Furthermore, local asymptotic stability of an equilibrium point is certain if and only if every eigenvalue* λ_n *of the Jacobian matrix* $J(\vec{h}) = \dfrac{\partial(\Phi_1, \Phi_2, ..., \Phi_n)}{\partial(h_1, h_2, ..., h_n)}$ *calculated at the equilibrium point satisfies* $|\arg(\lambda_n)| > \dfrac{\alpha\pi}{2}$.

Finally, Lemma 7 and Theorem 8 below will be used in the global stability analysis.

Lemma 7. *[9] Let* $h(t) \in \mathbb{R}^+$ *be a differentiable function. For any* $t > 0$ *and* $\alpha \in (0,1)$, *we have*

$$D^{\alpha}\left(h(t) - h^* - h^* \ln\frac{h(t)}{h^*}\right) = \left(1 - \frac{h^*}{h(t)}\right) D^{\alpha}h(t),\ h^* \in \mathbb{R}^+$$

Theorem 8. *[13] Let* L *be a positive function that is continuously differentiable and defined in the neighborhood* $\Theta(P^*)$ *of the equilibrium point* P^*. *As stated in LaSalle Invariance Principle,* P^**is asymptotically stable if*

1. $D^{\alpha}L(P) \le 0$ *for every* $P \in \Theta(P^*)$ *and*
2. *The set* $\{P \in \Theta(P^*) : D^{\alpha}L = 0\}$ *contains only* P^*.

In addition, if $L(P) \to \infty$ *while* $||P|| \to \infty$, *then* P^* *is globally asymptotically stable.*

3. Results and Discussion

We now present the basic analytical properties of Eq. (1) in the following subsection, which includes nonnegativity and boundedness of the solution, equilibrium points, basic reproduction number, and stability analysis. In the last subsection, we run numerical simulations to support the established analytical properties.

3.1. Nonnegativity and Boundedness of Solution

To preface, the solutions to Eq. (1) are $S(t)$, $E(t)$, $I(t)$, and $R(t)$, each representing the population of the respective compartment at time t. So, the solution must be nonnegative and bounded, as presented in the following proposition.

Proposition 9. *The solution of Eq. (1) is nonnegative for all* $t > 0$. *Furthermore, a positively invariant set of Eq. (1) is given by*

$$H = \left\{(S, E, I, R) \in \mathbb{R}^4 : 0 < S + E + I + R \le \frac{\Lambda}{\mu}\right\}.$$

where $\mathbb{R}^4$ *is a 4-dimensional space of real numbers.*

Proof. The SEIR model in Eq. (1) can be written as $D^\alpha W(t) = G(W)$ where

$$W = \begin{pmatrix} S \\ E \\ I \\ R \end{pmatrix}, G(W) = \begin{pmatrix} \Lambda - (\mu+\gamma)S - \beta SI + \omega I \\ \beta SI - (\delta+\mu)E \\ \delta E - (\tau+\mu+\omega)I \\ \gamma S + \tau I - \mu R \end{pmatrix}.$$

Similarly, in [8], $G(W)$ can be rewritten as $G(W) = A_1 + A_2 W + A_3 SW$ where

$$A_1 = \begin{pmatrix} \Lambda \\ 0 \\ 0 \\ 0 \end{pmatrix}, A_2 = \begin{pmatrix} -(\mu+\gamma) & 0 & \omega & 0 \\ 0 & -(\delta+\mu) & 0 & 0 \\ 0 & \delta & -(\tau+\mu+\omega) & 0 \\ \gamma & 0 & \tau & -\mu \end{pmatrix}, A_3 = \begin{pmatrix} 0 & 0 & -\beta & 0 \\ 0 & 0 & \beta & 0 \\ 0 & 0 & 0 & 0 \\ 0 & 0 & 0 & 0 \end{pmatrix}.$$

Thus, taking the norm of both sides of the equation and using triangular inequality, we have

$$||G(W)|| \leq ||A_1|| + (||A_2|| + ||A_3||||S||)||W||$$

As stated in Lemma 2, Eq. (1) has a unique solution for all $t \in [0, \infty)$. Subsequently, for each initial value $S(0) = 0$, $E(0) = 0$, $I(0) = 0$, and $R(0) = 0$, we have

$$\begin{aligned} D^\alpha S &= \Lambda + \omega I \geq 0, \\ D^\alpha E &= \beta SI \geq 0, \\ D^\alpha I &= \delta E \geq 0, \\ D^\alpha R &= \gamma S + \tau I \geq 0. \end{aligned}$$

Hence, by Lemmas 3–4, Eq. (1) with nonnegative initial values will have a nonnegative solution in $\mathbb{R}^4$. Next, by adding up each equation in Eq. (1), we have

$$D^\alpha N = \Lambda - \mu N \tag{2}$$

with $N = S + E + I + R$. Let Mittag-Leffler function be defined as in [14]. We introduce a Mittag-Leffler function $\mathcal{E}_\alpha(-\mu t^\alpha)$ where

$$\mathcal{L}\{\mathcal{E}_\alpha(-\mu t^\alpha)\} = \frac{s^{\alpha-1}}{s^\alpha + \mu}.$$

By using Lemma 5 on Eq. (2), we get

$$s^\alpha \mathcal{L}\{N(t)\} - s^{\alpha-1} N(0) = \frac{\Lambda}{s} - \mu \mathcal{L}\{N(t)\}.$$

Rearrange the equation so that we have the following form:

$$\mathcal{L}\{N(t)\} = \left(\frac{s^{\alpha-1}}{s^\alpha + \mu}\right)\left(N(0) - \frac{\Lambda}{\mu}\right) + \frac{\Lambda}{\mu s}.$$

Thus, by taking the inverse of the Laplace transformation, we have

$$N(t) = \mathcal{E}_\alpha(-\mu t^\alpha)\left(N(0) - \frac{\Lambda}{\mu}\right) + \frac{\Lambda}{\mu}.$$

Since in the context of fractional derivative we have $0 < \alpha \leq 1$, then $0 < \mathcal{E}_\alpha(-\mu t^\alpha) \leq 1$ according to the definition of Mittag-Leffler function, to which we can conclude that $N(t) \leq \frac{\Lambda}{\mu}$. □

3.2. Equilibrium Points

A state where a system is constant and remains unchanged, as long as there are no perturbations, is called an equilibrium point. Mathematically, equilibrium is reached when the rate of change of every state variable equals 0. Thus, the equilibrium points of Eq. (1) are achieved by solving

$$D^\alpha S = D^\alpha E = D^\alpha I = D^\alpha R = 0,$$

which results are two different equilibrium points. The first one is the Disease-Free Equilibrium (DFE), which occurs when the disease dies out, or mathematically, when $I = 0$. The other equilibrium is the Endemic Equilibrium, which occurs when the disease persists, or mathematically, $I \neq 0$. Let $P_0 = (S_0, E_0, I_0, R_0)$ be the DFE point. We have

$$P_0 = \left(\frac{\Lambda}{\mu + \gamma}, 0, 0, \frac{\Lambda\gamma}{\mu(\mu + \gamma)} \right).$$

Likewise, $P_1 = (S_1, E_1, I_1, R_1)$ is the Endemic Equilibrium point where

$$S_1 = \frac{(\delta + \mu)(\tau + \mu + \omega)}{\beta\delta}, E_1 = \frac{\tau + \mu + \omega}{\delta} I_1,$$
$$I_1 = \frac{\Lambda\beta\delta - (\mu + \gamma)(\delta + \mu)(\tau + \mu + \omega)}{\beta(\delta + \mu)(\tau + \mu) + \beta\mu\omega}, R_1 = \frac{\gamma S_1 + \tau I_1}{\mu}.$$

3.3. Basic Reproduction Number

Before we move on to stability analysis, we need to evaluate the basic reproduction number or $\mathcal{R}_0$. This number represents how many infection cases could occur from an infected individual in a completely susceptible population [15]. We proceed to calculate $\mathcal{R}_0$ by applying the Next Generation Matrix (NGM) method presented in [8], [15], where

$$\mathcal{F} = \begin{bmatrix} \beta SI \\ 0 \end{bmatrix}, \mathcal{V} = \begin{bmatrix} (\delta + \mu)E \\ -\delta E + (\tau + \mu + \omega)I \end{bmatrix}.$$

Let F and V respectively be the Jacobian matrices of $\mathcal{F}$ and $\mathcal{V}$, that is

$$F = \begin{bmatrix} 0 & \beta S \\ 0 & 0 \end{bmatrix}, V = \begin{bmatrix} (\delta + \mu) & 0 \\ -\delta & (\tau + \mu + \omega) \end{bmatrix}.$$

According to the NGM method, $\mathcal{R}_0$ is the spectral radius of FV^{-1}, which is

$$\mathcal{R}_0 = \frac{\Lambda\beta\delta}{(\mu + \gamma)(\delta + \mu)(\tau + \mu + \omega)}.$$

We can observe from the formula that $\mathcal{R}_0$ is directly proportional to parameters that contribute to infection cases such as β and Λ. We have $\frac{1}{(\tau + \mu + \omega)}$ as the average infectious time and $\frac{1}{(\mu + \gamma)}$ as the average time of susceptibility. The remaining $\frac{\delta}{\delta + \mu}$ is the probability that an exposed individual becomes infectious.

3.4. Local Stability Analysis

Now we are able to determine whether an equilibrium point is asymptotically stable or not by the value of $\mathcal{R}_0$. If an equilibrium point is asymptotically stable, then the system's state will progress towards that equilibrium. In this part, we discuss it locally, which applies to initial points in the neighborhood around equilibrium. It's important to note that from the local stability condition in Lemma 6, if $\mathrm{Re}(\lambda_n) < 0$ then

$$|\arg(\lambda_n)| > \frac{\pi}{2} \geq \frac{\alpha\pi}{2}, \ \alpha \in (0, 1],$$

This implies that any $\alpha \in (0,1]$ does not affect the local stability. Therefore, we present the equilibrium stability analysis as follows.

Theorem 10. *Local asymptotic stability of the Disease-Free Equilibrium P_0 is achieved if $\mathcal{R}_0 < 1$.*

Proof. The Jacobian matrix of Eq. (1) at P_0 is

$$\mathcal{J}(P_0) = \begin{bmatrix} -(\mu+\gamma) & 0 & -\dfrac{\Lambda\beta}{(\mu+\gamma)} + \omega & 0 \\ 0 & -(\delta+\mu) & \dfrac{\Lambda\beta}{(\mu+\gamma)} & 0 \\ 0 & \delta & -(\tau+\mu+\omega) & 0 \\ \gamma & 0 & \tau & -\mu \end{bmatrix}.$$

Consequently, the characteristic polynomial of $J(P_0)$ is

$$(\lambda+\mu+\gamma)(\lambda+\mu)(\lambda^2+c_1\lambda+c_2) = 0 \tag{3}$$

where $c_1 = (\delta+\mu)+(\tau+\mu+\omega)$ and $c_2 = (\delta+\mu)(\tau+\mu+\omega) - \dfrac{\Lambda\beta\delta}{\mu+\gamma}$. We have $\lambda_1 = -(\mu+\gamma)$ and $\lambda_2 = -\mu$, while the Routh-Hurwitz criterion for $\lambda^2 + c_1\lambda + c_2 = 0$ from Eq. (3) is satisfied if $c_1, c_2 > 0$. It is obvious that $c_1 > 0$ considering all the parameters are nonnegative, whereas $c_2 > 0$ if and only if $\mathcal{R}_0 < 1$. Hence, by Lemma 6, the local asymptotic stability of P_0 is proven. □

Theorem 11. *Local asymptotic stability of the Endemic Equilibrium P_1 is achieved if $\mathcal{R}_0 > 1$.*

Proof. Similar to the previous proof, the Jacobian matrix of Eq. (1) at P_1 is

$$\mathcal{J}(P_1) = \begin{bmatrix} -(\mu+\gamma) - \beta I_1 & 0 & -\beta S_1 + \omega & 0 \\ \beta I_1 & -(\delta+\mu) & \beta S_1 & 0 \\ 0 & \delta & -(\tau+\mu+\omega) & 0 \\ \gamma & 0 & \tau & -\mu \end{bmatrix}.$$

Consequently, the characteristic polynomial of $J(P_1)$ is

$$(\lambda+\mu)(\lambda^3 + (j+k+\ell)\lambda^2 + (jk+k\ell)\lambda + (\delta(\tau+\mu)+\mu j)\beta I_1) = 0 \tag{4}$$

where $j = \tau+\mu+\omega$, $k = \mu+\gamma+\beta I_1$, and $\ell = \delta+\mu$. We have $\lambda_1 = -\mu$, whereas the Routh-Hurwitz criterion for the equation $\lambda^3 + c_1\lambda^2 + c_2\lambda + c_3 = 0$ is satisfied if $c_1, c_2, c_3 > 0$ and $c_2c_1 - c_3 > 0$. Referring to Eq. (4), we have

$$c_1 = j+k+\ell,\ c_2 = jk+k\ell,\ c_3 = (\delta(\tau+\mu)+\mu j)\beta I_1.$$

It is obvious that $c_1, c_2, c_3 > 0$ and

$$\begin{aligned} c_2c_1 - c_3 &= (jk+k\ell)(j+k+\ell) - (\delta(\tau+\mu)+\mu j)\beta I_1 \\ &= k(j+\ell)(j+k+\ell) - (j\ell - \omega\delta)\beta I_1. \end{aligned}$$

By substituting the first k with $\mu+\gamma+\beta I_1$ and separating the terms that have βI_1, we have

$$\begin{aligned} c_2c_1 - c_3 &= (\mu+\gamma)(j+\ell)(j+k+\ell) + (j+\ell)(j+k+\ell)\beta I_1 - (j\ell-\omega\delta)\beta I_1 \\ &= (\mu+\gamma)(j+\ell)(j+k+\ell) + (j+\ell)^2\beta I_1 + k(j+\ell)\beta I_1 - j\ell\beta I_1 + \omega\delta\beta I_1. \end{aligned}$$

Thus, it can be observed that

$$c_2c_1 - c_3 = (\mu+\gamma)(j+\ell)(j+k+\ell) + (j^2+j\ell+\ell^2)\beta I_1 + k(j+\ell)\beta I_1 + \omega\delta\beta I_1 > 0.$$

Note that $\mathcal{R}_0 > 1$ is the sufficient condition for P_1 to exist and for the Routh-Hurwitz criterion to be satisfied. Hence, by Lemma 6, the local asymptotic stability of P_1 is proven. □

Remark 12. Local asymptotic stability of disease-free equilibrium can be interpreted as an early phase of an epidemic. When there are a few infected individuals and the reproduction number is below one, the disease will eventually die out. However, if the reproduction number is greater than one, even with a few infected individuals the disease can spread in the population.

3.5. Global Stability Analysis

In this subsection we proceed to analyze the system stability globally, which means we will discuss the system stability at $\mathbb{R}^4$, not just the neighborhood around equilibrium, in the following theorems.

Theorem 13. *Global asymptotic stability of the Disease-Free Equilibrium P_0 is achieved when $\mathcal{R}_0 \leq \dfrac{\mu}{\mu+\gamma}$.*

Proof. Let the Lyapunov function L_f be defined as

$$L_f(E,I) = \delta E + (\delta+\mu)I$$

The fractional derivative of L_f is given by

$$\begin{aligned} D^\alpha L_f &= \delta D^\alpha E + (\delta+\mu)D^\alpha I \\ &= \delta(\beta SI - (\delta+\mu)E) + (\delta+\mu)(\delta E - (\tau+\mu+\omega)I) \\ &= (\beta\delta S - (\delta+\mu)(\tau+\mu+\omega))I \\ &= \frac{\beta\delta}{\mathcal{R}_0}\left(\mathcal{R}_0 S - \frac{\Lambda}{\mu+\gamma}\right)I. \end{aligned}$$

By the positively invariant set H in Proposition 9, we have an upper bound of $\dfrac{\Lambda}{\mu}$. This also implies that $S \leq \dfrac{\Lambda}{\mu}$, which means

$$\mathcal{R}_0 S - \frac{\Lambda}{\mu+\gamma} \leq \mathcal{R}_0\left(\frac{\Lambda}{\mu}\right) - \frac{\Lambda}{\mu+\gamma}.$$

Since $\dfrac{\beta\delta}{\mathcal{R}_0}$ is positive, we can conclude that if $\mathcal{R}_0 \leq \dfrac{\mu}{\mu+\gamma}$ then $D^\alpha L_f \leq 0$.
Let H_f be the largest invariant set in $\{(S,E,I,R) : D^\alpha L_f = 0\}$. According to the definition of positively invariant set in [16] and Theorem 8, we can examine that $D^\alpha L_f = 0$ if and only if $I = 0$, which ultimately leads to $S \to S_0$, $E \to E_0$, and $R \to R_0$. Thus, the only element in H_f is P_0. By the LaSalle Invariance Principle, global asymptotic stability of P_0 is proven. □

Remark 14. It is important to note that the epidemic threshold remains $\mathcal{R}_0 = 1$. Theorem 13 raises a stronger sufficient condition because of the chosen Lyapunov function and the rough upper bound on S that is used in the proof. Therefore, it is possible that there exists a more intricate Lyapunov function or upper bound on S that gives a less restrictive condition for global asymptotic stability.

The global asymptotic stability of endemic equilibrium will be left unproven in this paper. However, we decided to share what we found on the Lyapunov function L_d given by

$$L_d(S,E,I) = S_1 f\left(\frac{S}{S_1}\right) + E_1 f\left(\frac{E}{E_1}\right) + aI_1 f\left(\frac{I}{I_1}\right).$$

where $f(x) = x - 1 - \ln(x)$, $x > 0$, and $a > 0$. The fractional derivative of L_d based on Lemma 7 is

$$\begin{aligned} D^\alpha L_d &\le \left(1 - \frac{S_1}{S}\right) D^\alpha S + \left(1 - \frac{E_1}{E}\right) D^\alpha E + a\left(1 - \frac{I_1}{I}\right) D^\alpha I \\ &= \left(\Lambda - (\mu+\gamma)S - \beta SI + \omega I - \frac{S_1(\Lambda - (\mu+\gamma)S - \beta SI + \omega I)}{S}\right) \\ &\quad + \left(\beta SI - (\delta+\mu)E - \frac{E_1(\beta SI - (\delta+\mu)E)}{E}\right) \\ &\quad + a\left(\delta E - (\tau+\mu+\omega)I - \frac{I_1(\delta E - (\tau+\mu+\omega)I)}{I}\right). \end{aligned}$$

Recall that $P_1 = (S_1, E_1, I_1, R_1)$ is an equilibrium point, which means that when $S = S_1$, $E = E_1$, $I = I_1$, and $R = R_1$ we have

$$\begin{aligned} D^\alpha S &= \Lambda - (\mu+\gamma)S_1 - \beta S_1 I_1 + \omega I_1 = 0, \\ D^\alpha E &= \beta S_1 I_1 - (\delta+\mu)E_1 = 0, \\ D^\alpha I &= \delta E_1 - (\tau+\mu+\omega)I_1 = 0, \\ D^\alpha R &= \gamma S_1 + \tau I_1 - \mu R_1 = 0. \end{aligned}$$

This brings out a relation of parameters that can be used. From $D^\alpha S$, we found out that $\Lambda = (\mu+\gamma)S_1 + \beta S_1 I_1 - \omega I_1$, which we substitute into the inequality to obtain the following.

$$\begin{aligned} D^\alpha L_d \le& (\mu+\gamma)S_1 + \beta S_1 I_1 - \omega I_1 - (\mu+\gamma)S + \omega I \\ &- \frac{S_1\left((\mu+\gamma)S_1 + \beta S_1 I_1 - \omega I_1 - (\mu+\gamma)S - \beta SI + \omega I\right)}{S} \\ &+ \left(\beta SI - (\delta+\mu)E - \frac{E_1\left(\beta SI - (\delta+\mu)E\right)}{E}\right) \\ &+ a\left(\delta E - (\tau+\mu+\omega)I - \frac{I_1\left(\delta E - (\tau+\mu+\omega)I\right)}{I}\right). \end{aligned}$$

Then from $D^\alpha E$ and $D^\alpha I$ we also found that $(\delta+\mu) = \dfrac{\beta S_1 I_1}{E_1}$ and $\delta = \dfrac{(\tau+\mu+\omega)I_1}{E_1}$. We choose specifically $a = \dfrac{\beta S_1}{\tau+\mu+\omega}$ then substitute all three which result in the expression below.

$$\begin{aligned} D^\alpha L_d \le& (\mu+\gamma)S_1 + \beta S_1 I_1 - \omega I_1 - (\mu+\gamma)S + \omega I - \frac{(\mu+\gamma)S_1^2}{S} - \frac{\beta S_1^2 I_1}{S} + \frac{\omega S_1 I_1}{S} + (\mu+\gamma)S_1 \\ &+ \beta S_1 I - \frac{\omega S_1 I}{S} + \left(-\frac{E_1 \beta SI}{E} + \beta S_1 I_1\right) + \left(-\beta S_1 I - \frac{I_1 \beta S_1 E I_1}{I E_1} + \beta S_1 I_1\right). \end{aligned}$$

All that's left is to rearrange the right-hand side by grouping it into three different terms that have either $(\mu+\gamma)S_1$, $\beta S_1 I_1$, or ω. The result is as follows:

$$D^\alpha L_d \le (\mu+\gamma)S_1\left(2 - \frac{S_1}{S} - \frac{S}{S_1}\right) + \beta S_1 I_1\left(3 - \frac{S_1}{S} - \frac{I_1 E}{I E_1} - \frac{S E_1 I}{S_1 E I_1}\right) + \omega\left(\frac{(S - S_1)(I - I_1)}{S}\right).$$

It can be checked by AM-GM inequality that

$$2 - \frac{S_1}{S} - \frac{S}{S_1} \leq 0, \text{ and } 3 - \frac{S_1}{S} - \frac{I_1 E}{I E_1} - \frac{S E_1 I}{S_1 E I_1} \leq 0.$$

However, the term $\omega \left(\frac{(S - S_1)(I - I_1)}{S} \right)$ has an indefinite sign. For this case, further rigorous calculations are needed to prove that $D^\alpha L_d \leq 0$.

3.6. Numerical Simulation

To support the analytical properties, we ran some simulations of Eq. (1). We conduct three simulations for three different cases with the parameter values given in Table 1.

Table 1: Parameter Values

Parameter	(i)	(ii)	(iii)	Reference
Λ	1	1	1	(i): Assumed; (ii) – (iii): [8]
μ	0.1	0.1	0.1	(i): [8]; (ii) – (iii): Assumed
β	0.3	0.3	0.5	[8]
γ	0.3	0.2	0.2	[8]
δ	0.2	0.2	0.3	Assumed
τ	0.4	0.2	0.4	(i) – (ii): [8]; (iii): Assumed
ω	0.2	0.01	[0.2, 0.5, 0.8]	[8]

This simulation uses $S(0) = 5$, $E(0) = 2$, $I(0) = 3$, and $R(0) = 1$ as initial values to illustrate a small population with people that are already infected. A few parameter values in Table 1 came from the previous research [8]. The remaining values are chosen through testing to ensure that we have the two plausible real-world scenarios as the result, either the disease dies out or persists. Parameter values in column (i) and (ii) represent the same level of disease transmission (β) but a different level of interventions (γ, τ, ω), while the parameter values in column (iii) are chosen specifically to observe the clearance rate (ω). Additionally, the parameter values for each fractional-order α are assumed to be the same so that we can observe the difference of each order value. The simulation will be held with the 2-stage Explicit Fractional Order Runge–Kutta (EFORK) method presented in [17].

3.6.1. Case 1: Stable Disease-Free Equilibrium Point

The first simulation uses the parameter values in column (i) of Table 1, with the result given in Fig. 1.

The basic reproduction number for this scenario is $\mathcal{R}_0 = 0.7143 < 1$. Previous analytical properties of the model implies that DFE, or in this case $P_0 = (2.5, 0, 0, 7.5)$, is asymptotically stable. It can be observed in Fig. 1 that the numerical solution corresponds with the analytical result. The value of (S, E, I, R) over the time converges towards P_0. It is also worth to mention that the solutions of Eq. (1) with smaller fractional-order α reach equilibrium first than models with larger α.

3.6.2. Case 2: Stable Endemic Equilibrium Point

For the second simulation, we apply parameter values in column (ii) of Table 1 with the result given in Fig. 2.

The basic reproduction number for this case is $\mathcal{R}_0 = 2.1505 > 1$. According to the analytical properties, Endemic Equilibrium or in this case $P_1 = (1.55, 1.822, 1.1758, 5.4516)$, is asymptotically stable. The result in Fig. 2 also suggests that the value of (S, E, I, R) converges towards P_1 when $t \to \infty$. Additionally, this simulation agrees with the aforementioned observation about fractional-order α. The solution of the model that uses $\alpha = 0.5$ reaches equilibrium before others

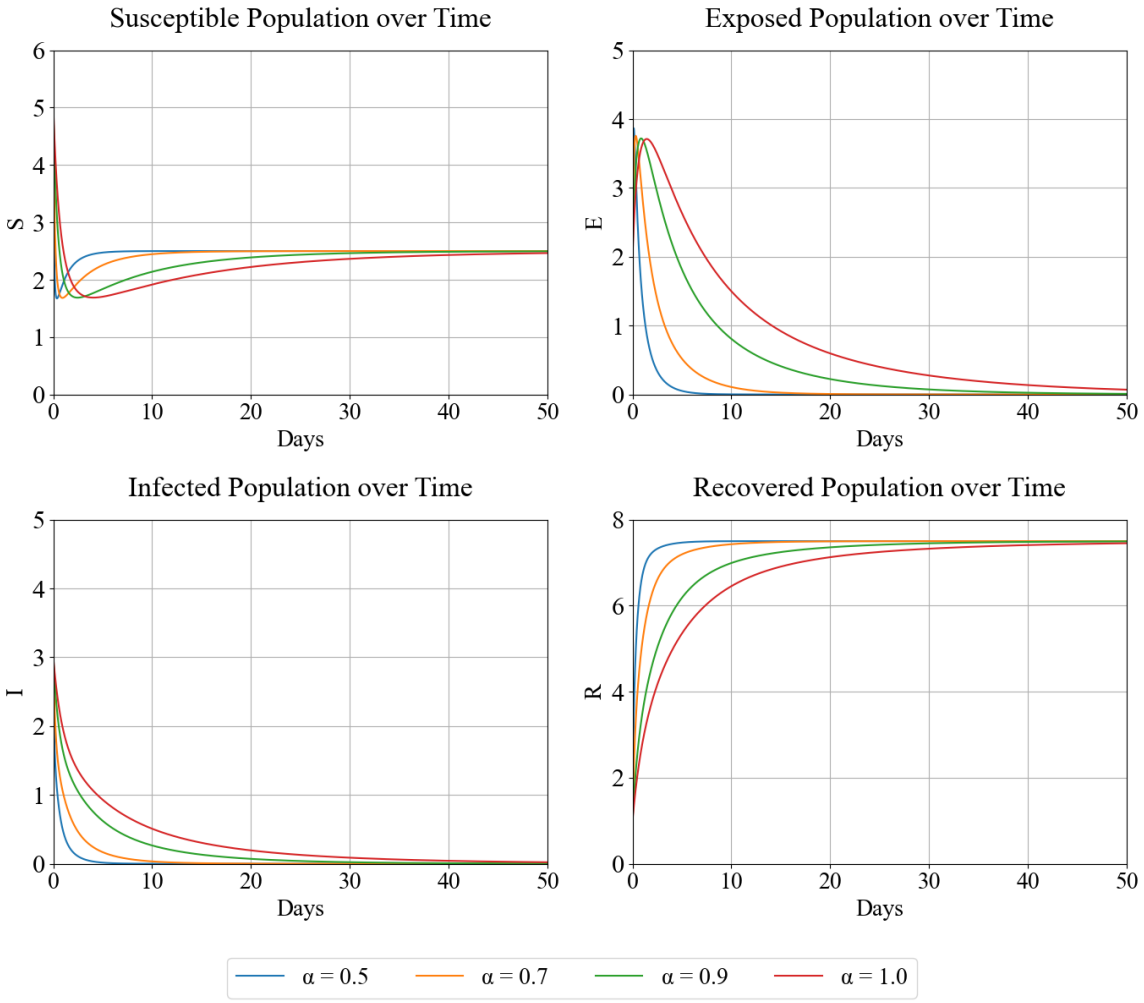

Fig. 1: Numerical solution illustrating the stability of disease-free equilibrium P_0 . It can be observed that the exposed and infected population (E and I) decreases to zero, indicating that the disease dies out, while the recovered population (R) increases. The susceptible population (S) also declines to a certain point and then stabilizes as the transmission of disease fades.

with higher α values. The results in both Fig. 1 and Fig. 2 show that the model dynamics are also dependent on the α value.

3.6.3. Case 3: Results with Different Clearance Rate

This last simulation is done to observe the impact of clearance rate on model dynamics using parameter values in column (iii) of Table 1 with $\alpha = 0.5$ and various ω values. The results are given in Fig. 3 with the basic reproduction numbers and asymptotically stable equilibrium points are presented in Table 2.

Table 2: Simulation Results for Different ω values

ω	$\mathcal{R}_0$	Asymptotically Stable Equilibrium Point
0.2	1.7857	$P_1 = (1.867, 1.4, 0.6, 6.1333)$
0.5	1.25	$P_1 = (2.67, 0.8, 0.24, 6.2933)$
0.8	0.9615	$P_0 = (3.33, 0, 0, 6.67)$

The result in Fig. 3 implies that clearance rate affects the model dynamic. Additionally, increasing the value of clearance rate ω is able to effectively decrease the number of infection cases. The individuals that return to susceptible are able to get vaccinated for immunity. It's

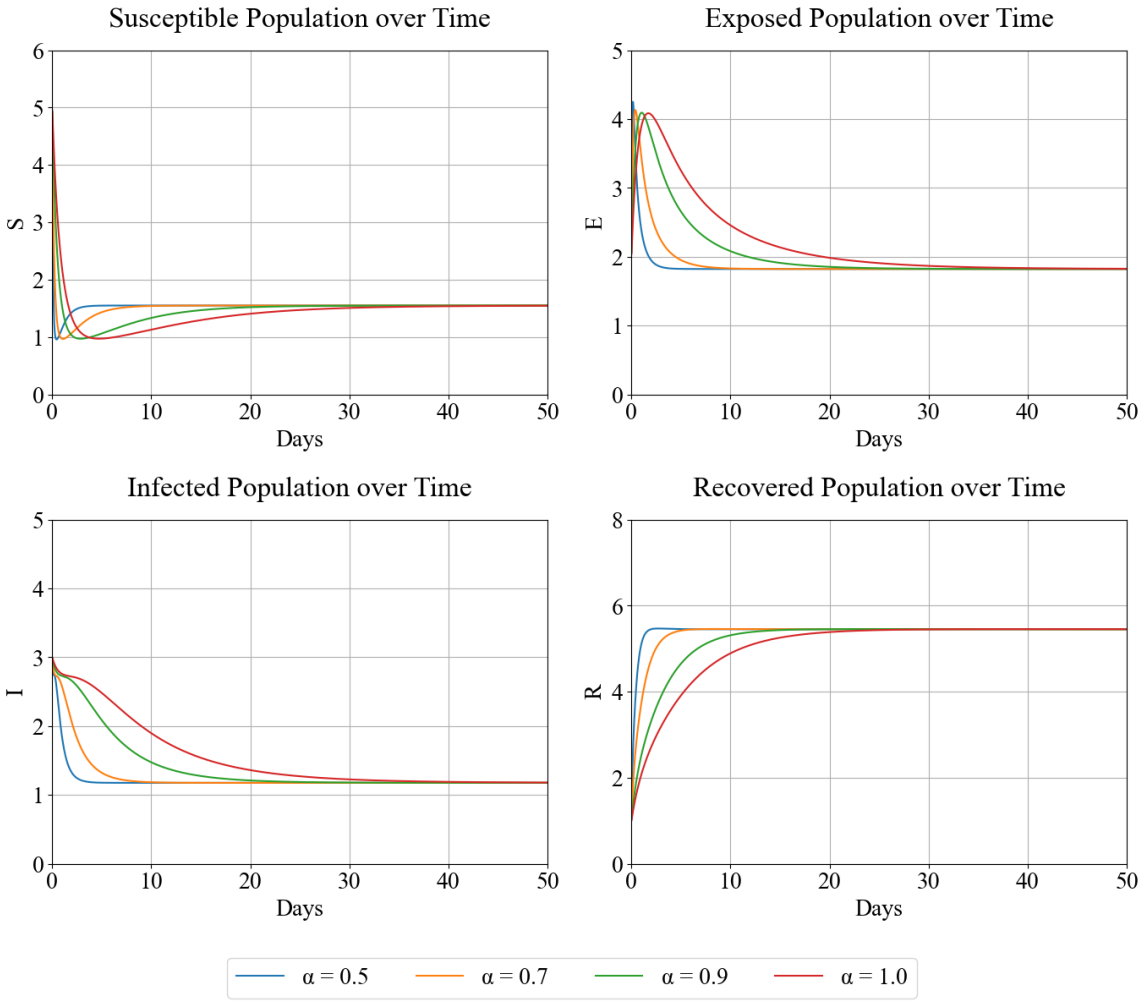

Fig. 2: Numerical solution illustrating the stability of endemic equilibrium P_1. It can be observed that the exposed and infected population (E and I) declines but stabilizes at a certain point, indicating that the disease persists. while the recovered population (R) still increases but not as many as the previous case. The susceptible population (S) also declines more before stabilizing because more individuals are exposed and infected.

shown that for $\omega = 0.8$, the infection cannot sustain itself and the disease slowly dies out. In a real-world setting, an increase in clearance rate can be achieved by improving the efficiency of giving early treatment to infected people, having them cleared from infection and getting vaccinated later on to prevent reinfection.

4. Conclusion

This paper discusses a fractional-order SEIR model that takes into consideration the infection clearance rate. We present the model formulation in Eq. (1) and show basic analytical properties, from nonnegativity and boundedness of solution to the stability of equilibrium points. Numerical simulations with the EFORK method validate the analytical properties presented. Results have shown that solution of the model differs depending on the value of the fractional-order α. Model with a smaller α value in the range of $0 < \alpha \leq 1$ has a solution that converges faster to equilibrium state. Furthermore, increasing the value of infection clearance rate effectively reduces the number of infection cases. Future research may involve more complex fractional-order epidemic models that use the concept of infection clearance, parameters estimated from real-world data, and the concept of spatial effects or stochastic models.

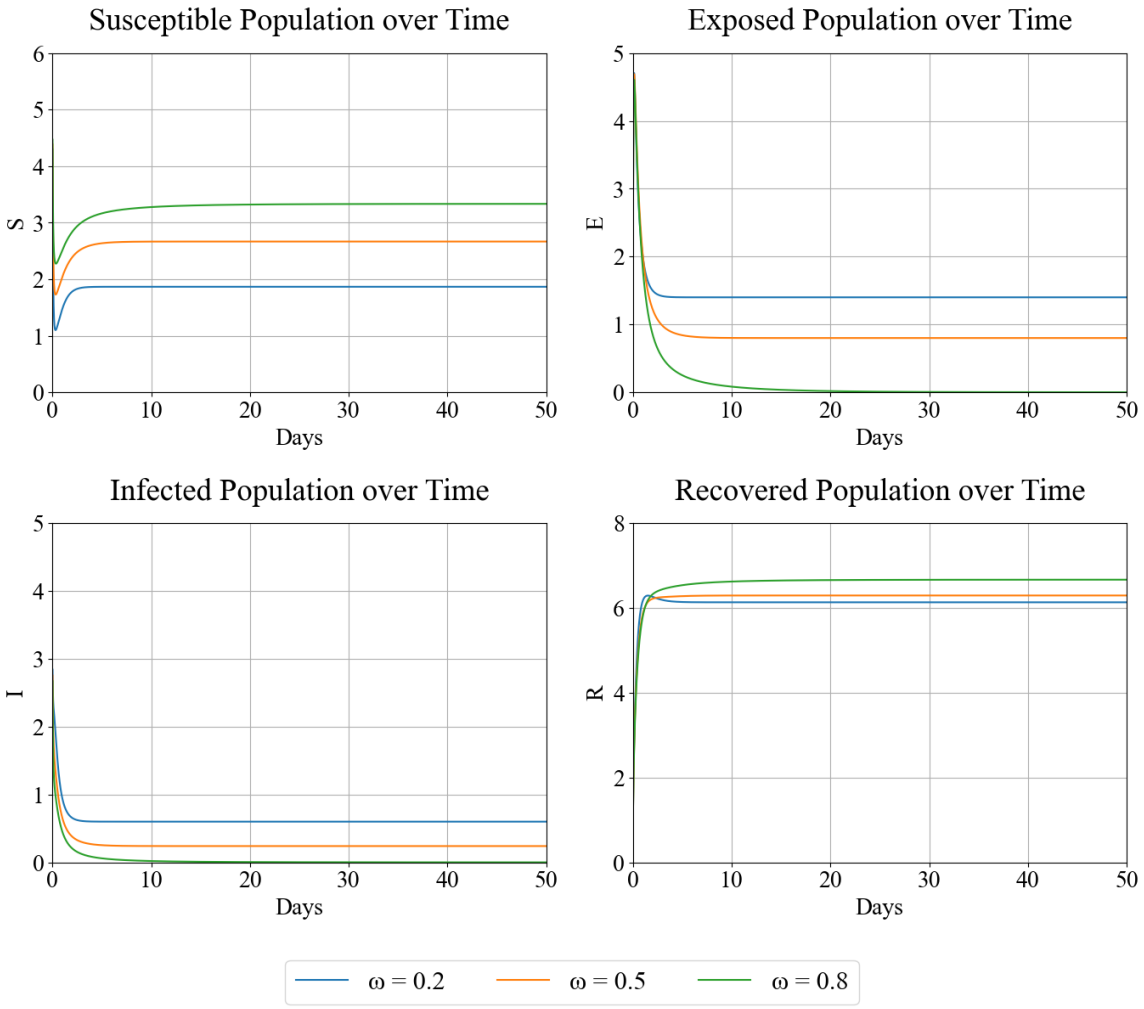

Fig. 3: Numerical solution with different clearance rate (ω) shows that increasing clearance rate effectively reduces the exposed and infected population (E and I), while the susceptible and recovered population (S and R) increases.

CRediT Authorship Contribution Statement

Author One: Conceptualization, Methodology, Software, Formal Analysis, Writing–Original Draft. **Author Two:** Writing–Review & Editing, Supervision. **Author Three:** Writing–Review & Editing, Supervision.

Declaration of Generative AI and AI-assisted technologies

No generative AI or AI-assisted technologies were used during the preparation of this manuscript.

Declaration of Competing Interest

The authors declare no competing interests.

Funding and Acknowledgments

This research was supported by LPPM Institut Teknologi Kalimantan, through an internal research grant. The authors gratefully acknowledge this support.

Data and Code Availability

The code used in numerical simulations is publicly available in the Github repository[1].

References

[1] World Health Organization, *The top 10 causes of death: Fact sheet*, https://www.who.int/news-room/fact-sheets/detail/the-top-10-causes-of-death, Accessed: 20-06-2025, 2024.

[2] World Health Organization, *Mpox*, https://www.who.int/news-room/fact-sheets/detail/mpox, Accessed: 20-06-2025, 2024.

[3] I. Korolev, "dentification and estimation of the SEIRD epidemic model for COVID-19," *Journal of Econometrics*, vol. 220, pp. 63–85, 2021. DOI: 10.1016/j.jeconom.2020.07.038.

[4] S. Mwalili, M. Kimathi, V. Ojiambo, D. Gathungu, and R. Mbogo, "SEIR model for COVID-19 dynamics incorporating the environment and social distancing," *BMC Research Notes*, vol. 13, Article number 352, 5 pages, 2020. DOI: 10.1186/s13104-020-05192-1.

[5] K. S. Nisar, M. Farman, M. Abdel-Aty, and J. Cao, "A review on epidemic models in sight of fractional calculus," *Alexandria Engineering Journal*, vol. 75, pp. 81–113, 2023. DOI: 10.1016/j.aej.2023.05.071.

[6] C. Yang and J. Wang, "A mathematical model for the novel coronavirus epidemic in Wuhan, China," *Mathematical Biosciences and Engineering*, vol. 17, no. 3, pp. 2708–2724, 2020. DOI: 10.3934/mbe.2020148.

[7] L. C. de Barros, M. M. Lopes, F. S. Pedro, E. Esmi, J. P. C. dos Santos, and D. E. Sánchez, "The memory effect on fractional calculus: an application in the spread of COVID-19," *Computational and Applied Mathematics*, vol. 40, Article number 72, 21 pages, 2021. DOI: 10.1007/s40314-021-01456-z.

[8] M. Sadki, S. Harroudi, and K. Allali, "Fractional-order sir epidemic model with treatment cure rate," *Partial Differential Equations in Applied Mathematics*, vol. 8, Article 100593, 9 pages, 2023. DOI: 10.1016/j.padiff.2023.100593.

[9] S. Paul, A. Mahata, S. Mukherjee, P. C. Mali, and B. Roy, "Dynamical behavior of fractional order SEIR epidemic model with multiple time delays and its stability analysis," *Examples and Counterexamples*, vol. 4, Article 100128, 13 pages, 2023. DOI: 10.1016/j.exco.2023.100128.

[10] A. Atangana and A. Secer, "A Note on Fractional Order Derivatives and Table of Fractional Derivatives of Some Special Functions," *Abstract and Applied Analysis*, vol. 2013, Article ID: 279681, 8 pages, 2013. DOI: 10.1155/2013/279681.

[11] A. Boukhouima, K. Hattaf, and N. Yousfi, "Dynamics of a Fractional Order HIV Infection Model with Specific Functional Response and Cure Rate," *International Journal of Differential Equations*, vol. 2017, no. 1, Article ID: 8372140, 8 pages, 2017. DOI: 10.1155/2017/8372140.

[12] N. Sene, "Analysis of the fractional SEIR epidemic model with Caputo derivative via resolvents operators and numerical scheme," *Discrete and Continuous Dynamical Systems - S*, vol. 18, no. 5, pp. 1316–1330, 2025. DOI: 10.3934/dcdss.2024149.

[13] E. M. Moumine, S. Khassal, O. Balatif, and M. Rachik, "Modeling and analysis of a fractional order spatio-temporal SEIR model: Stability and prediction," *Results in Control and Optimization*, vol. 15, Article 100433, 16 pages, 2024. DOI: 10.1016/j.rico.2024.100433.

[1] https://github.com/Iqbal-3z/Infection-Clearance-Rate-in-Fractional-Order-SEIR-Model-Stability-Analysis.git

[14] I. Batiha, S. Alshorman, I. Jebril, and M. A. Hammad, "A Brief Review about Fractional Calculus," *International Journal of Open Problems in Computer Science and Mathematics*, vol. 15, no. 4, 2022, https://www.researchgate.net/publication/366839100.

[15] C. Castillo-Garsow and C. Castillo-Chávez, "A Tour of the Basic Reproductive Number and the Next Generation of Researchers," in Cham: Springer International Publishing, 2020, pp. 87–124. DOI: 10.1007/978-3-030-33645-5_2.

[16] J. P. C. dos Santos, E. Monteiro, and G. B. Vieira, "Global stability of fractional SIR epidemic model," *Proceeding Series of the Brazilian Society of Computational and Applied Mathematics*, vol. 5, Article 010019, 7 pages, 2017. DOI: 10.5540/03.2017.005.01.0019.

[17] I. M. Batiha, A. A. Abubaker, I. H. Jebril, S. B. Al-Shaikh, K. Matarneh, and M. Almuzini, "A Mathematical Study on a Fractional-Order SEIR Mpox Model: Analysis and Vaccination Influence," *Algorithms*, vol. 16, Article 418, 18 pages, 9 2023. DOI: 10.3390/a16090418.